

Tenascin-W is a specific marker of glioma-associated blood vessels and stimulates angiogenesis *in vitro*

Enrico Martina,* Martin Degen,*¹ Curzio Rüegg,^{†,‡} Adrian Merlo,[§]
Maddalena M. Lino,[§] Ruth Chiquet-Ehrismann,* and Florence Brellier*²

*Friedrich Miescher Institute for Biomedical Research, Novartis Research Foundation, Basel, Switzerland; [†]Division of Experimental Oncology, Centre Pluridisciplinaire d'Oncologie, Centre Hospitalier Universitaire Vaudois, University of Lausanne, Lausanne, Switzerland; [‡]Swiss Institute for Experimental Cancer Research, NCCR Molecular Oncology, Epalinges, Switzerland; and [§]Laboratory of Molecular Neuro-Oncology, Department of Research, University Hospital, Basel, Switzerland

ABSTRACT The microenvironment hosting a tumor actively participates in regulating tumor cell proliferation, migration, and invasion. Among the extracellular matrix proteins enriched in the stroma of carcinomas are the tenascin family members tenascin-C and tenascin-W. Whereas tenascin-C overexpression in gliomas is known to correlate with poor prognosis, the status of tenascin-W in brain tumors has not been investigated so far. In the present study, we analyzed protein levels of tenascin-W in 38 human gliomas and found expression of tenascin-W in 80% of the tumor samples, whereas no tenascin-W could be detected in control, nontumoral brain tissues. Double immunohistochemical staining of tenascin-W and von Willebrand factor revealed that tenascin-W is localized around blood vessels, exclusively in tumor samples. *In vitro*, the presence of tenascin-W increased the proportion of elongated human umbilical vein endothelial cells (HUVECs) and augmented the mean speed of cell migration. Furthermore, tenascin-W triggered sprouting of HUVEC spheroids to a similar extent as the proangiogenic factor tenascin-C. In conclusion, our study identifies tenascin-W as a candidate biomarker for brain tumor angiogenesis that could be used as a molecular target for therapy irrespective of the glioma subtype.—Martina, E., Degen, M., Rüegg, C., Merlo, A., Lino, M. M., Chiquet-Ehrismann, R., Brellier, F. Tenascin-W is a specific marker of glioma-associated blood vessels and stimulates angiogenesis *in vitro*. *FASEB J.* 24, 778–787 (2010). www.fasebj.org

Key Words: neovascularization • secreted glycoproteins

TUMORIGENESIS HAS LONG BEEN considered as a cell-autonomous process. However, it is now well recognized that progressive steps of tumorigenesis are largely influenced by the tumor microenvironment (for reviews, see refs. 1–3). This microenvironment consists both of a rich extracellular matrix (ECM) called stroma and of all nontumoral cells populating the tumor, such as fibroblasts, macrophages, and endothelial cells. The stroma is mainly produced by mesenchymal cells and provides a physical support for tissue architecture. In

addition to this structural role, it also affects tumor cell behavior through activation of signaling pathways. Stroma associated with normal and tumor tissues strongly differ in their composition (for review, see ref. 4). For instance, being the site where tumor angiogenesis occurs, tumor stroma is on the one hand enriched in proangiogenic factors, such as vascular endothelial growth factor (VEGF) (5) and tumor necrosis factor alpha (TNF- α) (6), and on the other hand deprived of antiangiogenic factors, such as thrombospondin-1 (7). Unbalancing the preestablished equilibrium toward angiogenesis is crucial for the tumor, since these newly formed capillaries will supply oxygen and nutrients necessary for its expansion and growth.

Among the proteins known to be enriched in tumor stroma are members of the tenascin family. Tenascins are large extracellular glycoproteins participating in tissue modeling processes and are thus mainly expressed during embryogenesis. In adults, expression of tenascins becomes more restricted, at least in normal conditions (8). However, as with oncogenic proteins, two tenascin members can be reexpressed in tumors: tenascin-C and tenascin-W. Since its discovery 25 yr ago (9), many laboratories have confirmed the significance of tenascin-C as a tumor biomarker in various organs and have described its key role in tumorigenesis (for review, see ref. 10). Tenascin-C contributes to tumor development at many levels. First, it modulates the properties of tumor cells in terms of adhesion (9, 11), proliferation (9, 11), migration (12), and invasion (13). Sec-

¹ Present address: Department of Dermatology, Brigham and Women's Hospital, Harvard Skin Disease Research Center, Harvard Medical School, Boston, MA 02115, USA.

² Correspondence: Friedrich Miescher Institute for Biomedical Research, Novartis Research Foundation, Maulbeerstrasse 66, CH-4058 Basel, Switzerland. E-mail: florence.brellier@fmi.ch

This is an Open Access article distributed under the terms of the Creative Commons Attribution Non-Commercial License (<http://creativecommons.org/licenses/by-nc/3.0/us/>) which permits unrestricted non-commercial use, distribution, and reproduction in any medium, provided the original work is properly cited.

doi: 10.1096/fj.09-140491

ond, it stimulates tumor angiogenesis (14–18), and third, it is associated with the metastatic potential of cancer cells (19, 20). More recently characterized (21), tenascin-W constitutes a novel and efficient biomarker for human breast tumors (22) and colorectal tumors (23). Notably, and in contrast to tenascin-C, tenascin-W was undetectable in healthy colon tissues, suggesting that tenascin-W may have a better potential as a colon tumor biomarker.

In the present study, we focused on gliomas, which represent the most common primary brain tumors in humans. The characterization of gliomas depends on the type of cells from which they develop. Oligodendrogliomas are derived from oligodendrocytes and represent 4% of all brain tumors, while astrocyte-derived astrocytomas are much more common. Astrocytomas are graded from I to IV, the highest grade being also known as glioblastoma multiforme or glioblastoma. Patients suffering from glioblastoma, which are highly aggressive and invasive tumors, have a median survival time of only 10 mo. This very short survival time may be explained by the extreme adaptability of glioblastoma cells to antiproliferative or antiangiogenic treatments (for review, see ref. 24). In contrast, the median survival time for patients with oligodendroglioma is 10 yr (25).

Many studies have reported tenascin-C overexpression in brain tumors (for review, see refs. 26, 27). Tenascin-C levels are higher in glioblastoma than in oligodendroglioma (28). High expression levels of perivascular tenascin-C in glioma were shown to correlate with shorter progression-free survival (12), and expression of stromal tenascin-C was shown to be increased in higher tumor grades with poor prognosis (29). In contrast, nothing is known concerning the status of tenascin-W in these tumors.

Because the key role played by tenascin-C in brain tumorigenesis made it a recognized target for glioma treatment (30), we tested whether tenascin-W expression correlates with tumorigenesis in the brain as well, and we investigated its potential function during glioma development.

MATERIALS AND METHODS

Glioma biopsies

Gliomas, as well as healthy control brain samples, were obtained from the University Hospital of Basel in accordance with the guidelines of the ethical committee of the University of Basel. Glioblastoma samples were from patients aged 39 to 84 yr (mean age 60 yr), astrocytomas from patients aged 40 to 63 (mean age 45 yr) and oligodendrogliomas from patients aged 38 to 67 (mean age 57 yr). Healthy control samples were obtained from independent individuals. One part of each biopsy was used for protein extraction, and another part was embedded in optimal cutting temperature (OCT) compound (Tissue Tek; Miles Laboratories, Naperville, IL, USA) for the preparation of cryosections. Tumors were diagnosed and graded according to the World Health Organization classification of tumors of the nervous system.

Western blot analysis

Tissue samples were thawed on ice, minced, and homogenized in RIPA lysis buffer. After measuring the protein concentration with the Bio-Rad protein assay (Bio-Rad, Munich, Germany), samples were separated by SDS-PAGE (6%) and electroblotted to polyvinylidene difluoride membranes (Millipore, Billerica, MA, USA). Equal protein loading was confirmed by staining the membrane with amido black. After a blocking step in 5% milk, membranes were incubated overnight with the rabbit polyclonal antiserum pAb (3F/4) raised against human tenascin-W (1:750) (22), the mouse monoclonal antibody B28-13 raised against human tenascin-C (1:100), a mouse monoclonal antibody against vinculin (V-9131; 1:2000; Sigma, Schnellendorf, Germany), or a rabbit polyclonal antibody against actin (1:2000; A-5060, Sigma). They were then incubated for 1 h with anti-mouse IgG or anti-rabbit IgG coupled to horseradish peroxidase. Blots were developed using Super Signal (Pierce, Rockford, IL, USA) for tenascin-C and tenascin-W and ECL reagent (GE Healthcare, Otelfingen, Switzerland) for vinculin and actin. They were then exposed to Kodak BioMax MR Films (Kodak, Rochester, NY, USA).

Omnibus database search

Using the Gene Expression Omnibus database in PubMed, we imported the values corresponding to *tenascin-W* (found as “*tenascin N*”) of the dataset record GDS1813. This dataset was generated to study gliomagenesis by analyzing a set of 50 human gliomas of various histogenesis (31). The values imported from the dataset correspond to the ratio between values obtained for each sample and those obtained for a common human reference, expressed in binary logarithm (see Supplemental Table 1). The ratio was then calculated in a linear basis for each sample (see Supplemental Table 1) or as a mean for each disease state (see **Table 1**). The “fold change over normal” is the ratio between the mean values found in each disease state and in the normal brain.

Immunostaining

Chromogenic and fluorescent detection was performed on 9- or 12- μm -thick cryosections using the Discovery XT automated stainer (Ventana Medical Systems, Tucson, AZ, USA) with a standard and a customized procedure, respectively. Frozen tissue slides were dried for 1 h at room temperature, fixed for 10 min at -20°C in acetone, and then introduced into the automate. For chromogenic stainings, slides were incubated for 1 h at 37°C with the mouse monoclonal 56O antibody raised against human tenascin-W (1:1000) (23), the B28-13 antitenascin-C antibody (1:1000), or a rabbit polyclonal antibody against von Willebrand factor (1:25,000; A0082, Dako Corp., Carpinteria, CA, USA). They were then treated for 32 min at 37°C with a biotinylated anti-mouse or anti-rabbit secondary antibody (1:200; 715-065-150 and 711-065-152, respectively; Jackson ImmunoResearch Laboratories, West Grove, PA, USA) and developed with the DAB Map detection kit (Ventana). Counterstainings were obtained with hematoxylin and bluing reagent (Ventana). For immunofluorescence stainings, slides were incubated for 1 h at 37°C with anti-tenascin-W mAb 56O (1:50), anti-tenascin-C mAb B28-13 (1:50), anti-von Willebrand factor (1:200), rabbit polyclonal anti-desmin antibody (1:100, RB-9014-P1, Neomarkers, Fremont, CA, USA), or rabbit polyclonal anti-laminin antibody (1:200; Life Technologies, Gaithersburg, MD, USA). The slides were then treated for 32 min at 37°C with Alexa Fluor 488 donkey anti-mouse IgG and Alexa Fluor 568 donkey anti-rabbit IgG or Alexa Fluor 647 goat anti-rabbit IgG

secondary antibodies (1:200; A21202, A10042, and A21245, respectively; Invitrogen, Basel, Switzerland), carefully rinsed by hand, and mounted with prolong gold reagent (Invitrogen). Wide-field images were acquired using a Zeiss Axiovert 200 microscope equipped with a charge-coupled device Cool Snap HQ camera, using a $\times 20/0.50$ or a $\times 40/1.3$ oil objective (Carl Zeiss, Oberkochen, Germany). Confocal laser scanning microscopy was performed using a Zeiss AxioPlan 2-LSM510meta, using a $\times 63/1.4$ oil objective. Images were processed using ImageJ software (<http://rsb.info.nih.gov/ij/>).

Cell culture

Human umbilical vein endothelial cells (HUVECs) were a kind gift of Grégory Bieler (Division of Experimental Oncology, University of Lausanne). The cells were isolated from 3 independent umbilical cords and pooled. HUVECs were cultured in endothelial growth medium consisting of medium 199 (Life Technologies) supplemented with 10% FCS (Hyclone, Lausanne, Switzerland), 12 $\mu\text{g}/\text{ml}$ bovine brain extract (Clonetics, Walkersville, MD, USA), 10 ng/ml human recombinant EGF (Peprotech, Rocky Hill, NJ, USA), 25 U/ml heparin (Sigma), 1 $\mu\text{g}/\text{ml}$ hydrocortisone (Sigma), 2 mM L-glutamine, 100 U/ml streptomycin, and 100 U/ml penicillin. Cells were used between passages 4 and 8.

Human embryonic kidney-293 (HEK-293) cells used in this study were either mock transfected or transfected to stably express His-tagged full-length human tenascin-W (22), His-tagged full-length human tenascin-C (32) or His-tagged EGF-repeats of human teneurin-4 (D. Kenzelmann, unpublished data). HEK-293 cells were cultured in DMEM/10% FCS with 2 $\mu\text{g}/\text{ml}$ puromycin.

Purification of tenascins and fibronectin

HEK-293 cells stably transfected to express either His-tagged human tenascin-W or His-tagged human tenascin-C were grown to confluence. Serum-free culture medium containing the secreted recombinant human tenascins was collected, and after ammonium sulfate precipitation (0–38%) and dialysis against PBS containing 0.01% Tween-20, the protein was passed over a gelatin-agarose column to remove fibronectin, followed by affinity purification on an Ni-NTA resin (Invitrogen) in the presence of 0.5 M urea, as described previously (22). The protein eluates were then dialyzed against PBS containing 0.01% Tween using 100-kDa-cutoff dialysis bags (Spectrumlabs, Greensboro, NC, USA) to limit potential copurification of small molecules. Purified tenascins appeared as single bands on Coomassie-stained acrylamide gels. Fibronectin was purified from horse serum as described previously (33).

Cell adhesion assay

Seventy-two-well MicroWell Mini Trays (Nunc, Roskilde, Denmark) were coated for 90 min at 37°C with 10 μl /well of 20 $\mu\text{g}/\text{ml}$ of rat tail collagen type I (BD Biosciences, San Jose, CA, USA). After 3 washes with PBS, the wells were coated overnight at 4°C with PBS containing 0.01% Tween, 200 ng of human tenascin-W, human tenascin-C, or fibronectin. The wells were blocked for 1 h at room temperature with PBS containing 1% BSA. HUVECs were trypsinized and resuspended in serum-free medium, and 1500 cells were seeded in each well. For the dose-response experiment, wells were coated with collagen and washed and blocked with BSA. Cells were then seeded in serum-free medium containing a different concentration of soluble tenascin-W, or BSA as a control. After 3 h at 37°C, cells were washed 3 times with PBS, fixed with 4% formaldehyde, and stained with 0.1% crystal violet.

Pictures of the entire wells were taken at $\times 2.5$ under an inverted microscope, and the cells were counted. The ratio between the number of elongated cells and the total number of cells was calculated. Experiments were done in triplicate wells, in 3 independent experiments.

Cell motility assay

Twenty-four-well plates were coated as described above. HUVECs were trypsinized and resuspended in serum-free medium, and 5×10^4 cells were seeded in each well. Cells were allowed to adhere for 2 h at 37°C. Time-lapse microscopy was then performed using an inverted microscope with a $\times 5$ objective, acquiring a picture every 10 min for 10 h. During this time, the plate was maintained at 37°C in 6% CO_2 and 100% humidity. Cell motility was quantified manually, tracking ≥ 35 cells/condition throughout the time stack, using the ImageJ software. The experiment was repeated twice.

Generation of spheroids

Spheroids of HEK-293 cells and HUVECs were prepared, as described previously, as “random” and “standard” spheroids, respectively (34). HEK-293 cells were labeled with fluorescent vibrant dye DiL (Invitrogen), trypsinized, and resuspended in DMEM/10% FCS containing 0.42% (w/v) carboxymethylcellulose. Three million cells were seeded in a nonadherent Petri dish for bacterial culture and incubated overnight at 37°C. Under these conditions, cells aggregate spontaneously to form random spheroids of similar sizes. To obtain HUVEC spheroids of defined size and cell number (standard spheroids), subconfluent monolayers of HUVECs were labeled with the fluorescent vibrant dye DiO (Invitrogen), trypsinized, and resuspended in endothelial growth medium containing 0.24% (w/v) carboxymethylcellulose (Sigma). Four hundred cells were seeded in each well of a nonadherent round-bottom 96-well plate (Greiner Bio-One, St. Gallen, Switzerland) to form spheroids, which were collected the next day.

Spheroid sprouting assay

An *in vitro* angiogenesis assay described previously (35) was adapted as follows: HUVEC spheroids were transferred into a rat type I collagen gel (1.2 mg/ml), containing purified tenascin-W, purified tenascin-C, or BSA at a final concentration of 20 $\mu\text{g}/\text{ml}$. In coculture experiments, HEK-293 cells expressing tenascin-W, tenascin-C, or an unrelated teneurin-4 fragment, or mock-transfected HEK-293 cells were incorporated into the gel either as single cells (8000 cells/ml gel) or as random spheroids (250 μl random spheroid suspension/ml gel). The fluid spheroid-containing gel was transferred into prewarmed 24-well suspension plates (Greiner Bio-One) and incubated for 30 min at 37°C. After polymerization of the gel, spheroids were fed with 100 μl of endothelial growth medium, with or without 10 ng/ml of VEGF-165 (R&D Systems, Minneapolis, MN, USA) and incubated for 48 h at 37°C. For each condition, pictures of 10 spheroids were acquired under an inverted microscope at $\times 100$ and analyzed. Cumulative sprout length (CSL) was quantified by measuring the total length of all sprouting processes originating from each single spheroid, using the ImageJ software. Three independent experiments were performed.

RESULTS

Brain tumors overexpress tenascin-W

We first assessed tenascin-W and tenascin-C protein content in extracts of normal brain by immunoblot analysis.

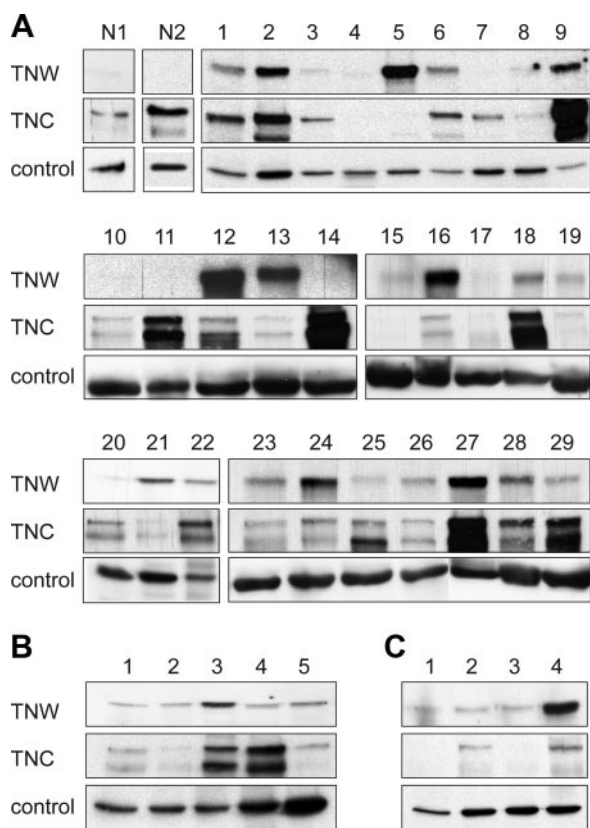


Figure 1. Immunoblot analysis of tenascin-W and tenascin-C expression in glioma protein extracts. Protein extracts of glioma or healthy brain tissues were separated by SDS-PAGE and immunoblotted for tenascin-W and tenascin-C. Blots were also probed for actin or vinculin to check equal loadings of the samples. **A)** Healthy brain tissue extracts (N1 and N2) and glioblastoma extracts (lanes 1–29). **B)** astrocytoma extracts (lanes 1–4). **C)** Oligodendroglioma extracts (lanes 1–4). Note the absence of tenascin-W in healthy brain tissues. In contrast, the majority of the glioma extracts show expression of tenascin-W. Tenascin-C is also expressed in most of the glioblastomas and astrocytomas, but much less in oligodendrogliomas. Tenascin-C is also detectable in healthy brain tissues.

No tenascin-W could be detected in normal brain, while tenascin-C was present (**Fig. 1A**, lanes N1 and N2). We then analyzed 29 glioblastoma samples. Almost all samples contained tenascin-C, as well as tenascin-W at various levels (**Fig. 1A**, lanes 1–29). We could detect tenascin-W in 21 extracts (*i.e.*, >70% of the samples) and among them,

8 expressed tenascin-W at high or very high levels. We also analyzed tenascin-W and tenascin-C expression in 5 astrocytomas and 4 oligodendrogliomas (**Fig. 1B, C**). Tenascin-W was present in all of these samples tested. In contrast to tenascin-C, which is overexpressed in glioblastoma and astrocytomas, but not in oligodendrogliomas (as described previously in ref. 28), no glioma subtype specificity for tenascin-W expression was observed. Altogether, ~80% of the glioma samples tested were tenascin-W-positive.

Using the Gene Expression Omnibus database accessible on PubMed, we extracted raw transcript data from a transcript profiling study of gliomas by Bredel *et al.* (31). This revealed that 27 of the 30 glioblastoma samples tested showed overexpression of *tenascin-W* mRNA compared to 4 healthy brain samples (see Supplemental Table 1). The fold change increase in *tenascin-W* transcript level between healthy brain and glioblastoma was almost 2.5 (Table 1). This increase was statistically significant ($P < 0.05$, ANOVA test), thereby confirming our protein expression data at the RNA level and in an independent dataset.

Blood vessels in brain tumors are stained for tenascin-W

To identify the cellular source of tenascin-W in gliomas, we performed immunohistochemical analyses on glioblastoma and oligodendroglioma cryosections. Tenascin-W immunostaining revealed circular structures histologically reminiscent of blood vessels, similarly to tenascin-C, which, in addition, was present around the glioblastoma cells throughout the tissue section (**Fig. 2**). We then costained the sections for the tenascins and von Willebrand factor, an established marker of blood vessels. We observed complete overlap between tenascin-W immunostaining and blood vessel structures marked by von Willebrand factor (**Fig. 3C, E**), suggesting that the cellular source of tenascin-W could be tumor endothelial cells. Immunohistochemical analyses of healthy brain tissues showed, as expected, a typical, sparser network of blood vessels compared to tumor tissues. Consistent with our immunoblot analyses, tenascin-W was not detectable in healthy brain tissue, even around vessels (**Fig. 3A**), suggesting that tenascin-W expression is tumor-endothelial specific. Tenascin-C and von Willebrand double staining showed only a partial overlap, as the tenascin-C staining

TABLE 1. *Tenascin-W* levels in an independent RNA profiling

| Disease state | Tenascin-W mRNA level (tissue of interest/common reference) | Fold change over normal |
|---------------------------------------|--|----------------------------|
| Normal ($n=4$) | 0.745 ± 0.093 | 1 |
| Oligodendroglioma ($n=8$) | 0.969 ± 0.061 | 1.3 |
| Anaplastic oligoastrocytoma ($n=6$) | 0.992 ± 0.093 | 1.3 |
| Glioblastoma ($n=30$) | 1.831 ± 0.188 | 2.5* |
| Astrocytic tumors ($n=4$) | 1.305 ± 0.437 | 1.8 |
| Glioneuronal neoplasm ($n=1$) | 1.496 | 2 |

n = number of samples in each category. * $P < 0.05$; ANOVA test.

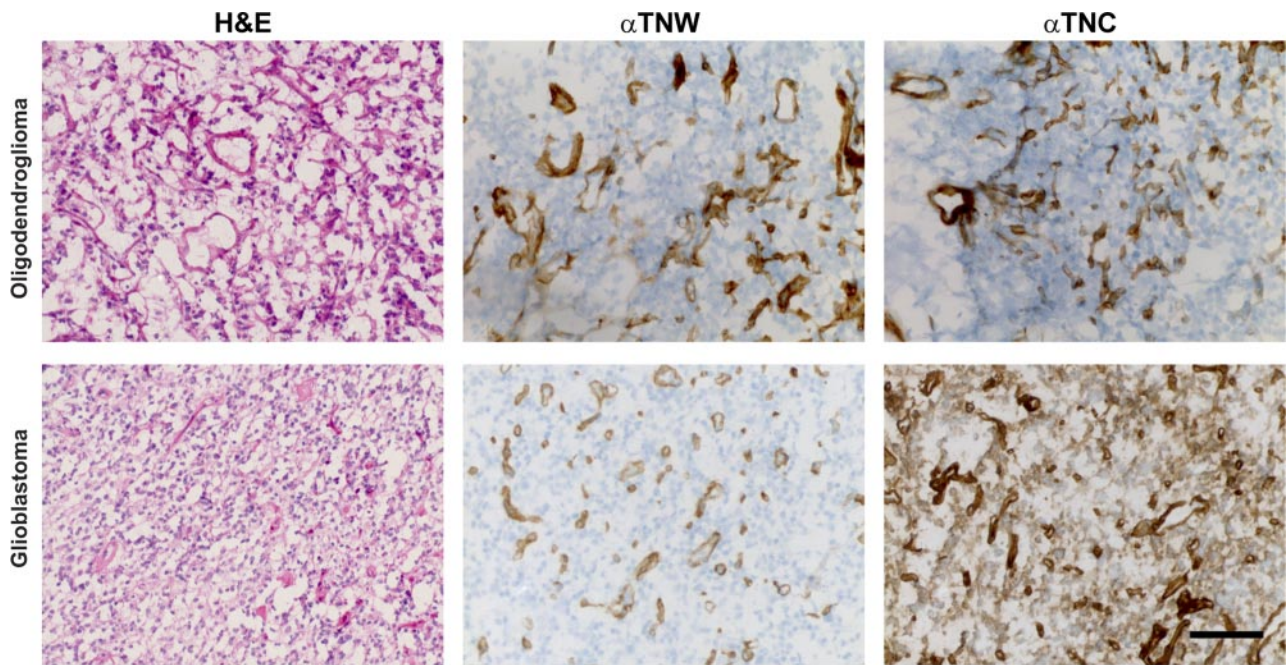


Figure 2. Immunohistochemical detection of tenascin-W and tenascin-C in gliomas. Cryosections of oligodendroglioma (top panels) and glioblastoma (bottom panels) were stained with hematoxylin and eosin (H&E), as well as with tenascin-W (α TNW) and tenascin-C (α TNC) antibodies. Cell nuclei are counterstained in blue in middle and right panels. Note the circular structures, reminiscent of blood vessels, stained by tenascin-W and tenascin-C. In glioblastoma, tenascin-C stains all cells throughout the section, while tenascin-W is present only in the vessel-like structures. Scale bar = 50 μ m.

mainly surrounded the staining for von Willebrand factor (Fig. 3D, F). Tenascin-C may thus not be secreted solely by the endothelial cells themselves. In healthy brain tissue sections, tenascin-C remained undetectable (Fig. 3B), suggesting that tenascin-C may not be expressed in the entire brain.

To assess more precisely the localization of tenascin-W, we then stained sections of glioblastoma with anti-desmin and anti-pan-laminin antibodies. The former is known to stain pericytes at the periphery of blood vessels, and the latter stains the basement membrane shared by the endothelial and surrounding pericyte cell layers. Tenascin-W staining was adjacent to desmin staining and rarely enclosed the pericytes (a typical picture is shown in Fig. 4A), in contrast to tenascin-C, which clearly enclosed all the pericytes surrounding the blood vessels (Fig. 4B). Furthermore, tenascin-W staining was restricted to the area delimited by the laminin staining (Fig. 4C), whereas tenascin-C staining clearly extended beyond the periphery of the basement membrane (Fig. 4D). These experiments show that tenascin-W is present in and around the endothelial cell layer but does not overlap with the pericyte cell layer.

Tenascin-W promotes elongation and migration of endothelial cells

A characteristic feature of angiogenic endothelial cells is their migratory capacity associated with the acquisition of an elongated cell shape (36). To investigate whether tenascin-W influences the morphology of endothelial

cells, we compared HUVECs seeded on collagen substrata, including tenascin-W, tenascin-C, or fibronectin. Cells seeded in serum-free conditions on a mixture of collagen I/fibronectin were polygonal and well spread, with a regular cobblestone-like shape (Fig. 5A, left panel). When the cells were cultured on collagen I/tenascin-C or collagen I/tenascin-W mixtures, a fraction of the cells exhibited an elongated cell shape. The cells were mostly bipolar with long, thin, protrusions (Fig. 5A, middle and right panels), a morphology reminiscent of migrating cells. The number of elongated cells was significantly higher in the presence of tenascin-C and tenascin-W than in the presence of fibronectin (Fig. 5B), suggesting that tenascin-W, as it has been shown before for tenascin-C (17), promotes endothelial cell elongation. When used in solution rather than coated on the surface, tenascin-W triggered a similar change of morphology. It increased the proportion of elongated HUVECs with an EC_{50} of 2.5 μ g/ml and reached a maximal effect at 20 μ g/ml concentration (Fig. 5C), which was used subsequently in all experiments.

The typical morphology of HUVECs when cultured on a mixed collagen I/tenascin-W substratum suggested that these cells may acquire a motile phenotype in the presence of tenascin-W (37). To test this hypothesis, we tracked the movement of the cells by live imaging over a period of 10 h. On each substratum tested, we observed random movements of the cells. When we measured the mean speed of HUVECs, we observed a higher speed on collagen I/tenascin-W and collagen I/tenascin-C compared to collagen I/fibronectin (Fig. 5D). Cell speed comparisons between

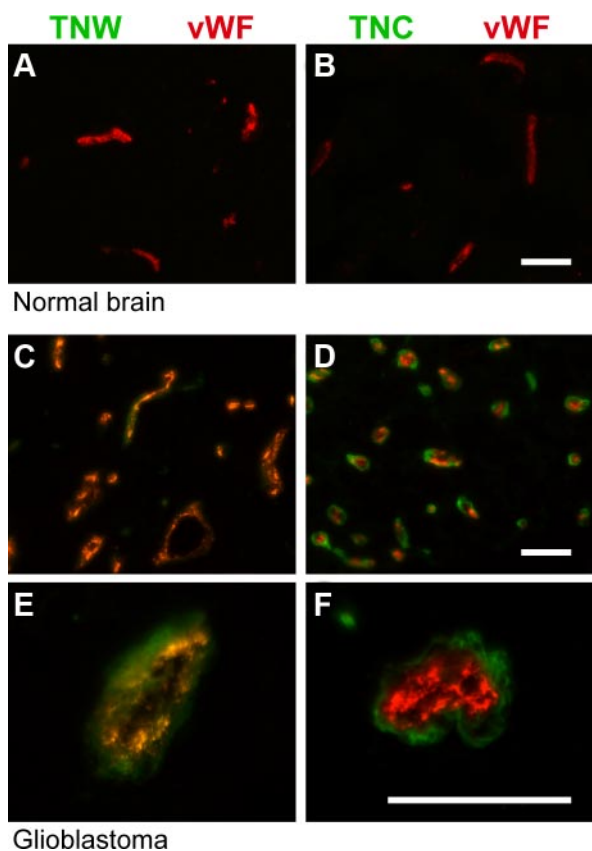


Figure 3. Double immunofluorescence staining of tenascin-W or tenascin-C with von Willebrand factor in normal brain and glioblastoma. Cryosections of control brain (A, B) and glioblastomas (C–F) were used for fluorescent detection of tenascin-W (TNW; green; A, C, E), tenascin-C (TNC; green; B, D, F) and von Willebrand factor (vWF; red). Note the normal, typical network of capillaries in normal brain (A, B), compared to the dense network observed in glioblastomas (C, D). There is a complete overlap between TNW and vWF stainings (E), in contrast to the partial overlap between TNC and vWF (F). Scale bars = 50 μm .

collagen I/fibronectin *vs.* collagen I alone revealed no difference (data not shown). Although a large heterogeneity between individual cells within each condition was observed, statistical analyses confirmed a significant effect of tenascin-C and tenascin-W on the motility of HUVECs ($P < 0.0001$, ANOVA test).

Tenascin-W promotes endothelial cell sprouting

To collect further evidence for a potential angiogenic activity of tenascin-W, we monitored its effect on the endothelial sprouting capacity of HUVECs, using a collagen gel-embedded spheroid-based *in vitro* angiogenesis assay. Incorporation of tenascin-C into the gel promoted endothelial cell sprouting, as described previously (38). Similarly, when HUVEC spheroids were incorporated in a tenascin-W-containing gel, we observed a significant induction of endothelial cell sprouts (Fig. 6A, top panels). The extensions formed by the sprouting cells were similar to the ones triggered by tenascin-C. The measurement of the CSLs confirmed

the increase in the presence of tenascin-W and tenascin-C to be statistically significant (Fig. 6B, open bars). Interestingly, the addition of VEGF, a potent proangiogenic factor, further increased the HUVEC sprouting capacities triggered by tenascin-C and tenascin-W (Fig. 6A, bottom panels; B, solid bars), suggesting an additive effect of tenascins and VEGF.

To exclude the possibility of an indirect effect mediated by contaminating proangiogenic factors copurified with tenascins, we established a coculture system. We cultured HUVEC spheroids in the presence of stably transfected HEK-293 cells as a source of tenascin-W, tenascin-C, or a teneurin-4 fragment, the latter serving as a negative control. Simultaneous incorporation in the gel of independently prepared HUVEC spheroids labeled with a green vital dye and HEK-293 spheroids labeled in red led to the formation of HUVEC sprouting in the presence of VEGF, only when the HEK-293 spheroids were expressing tenascin-C or tenascin-W (Fig. 7A). For quantification, we prepared collagen gels populated with dissociated HEK-293 cells and measured the CSL of HUVEC spheroids under each condition. The presence of HEK-293 cells secret-

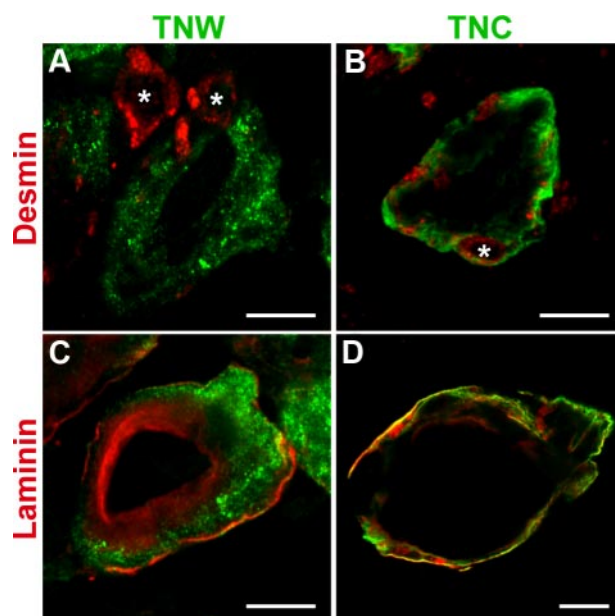


Figure 4. Double immunofluorescence staining of tenascin-W or tenascin-C with desmin and laminin in glioblastoma. Cryosections of glioblastomas were used for fluorescent detection of tenascin-W (TNW; green; A, C), tenascin-C (TNC; green; B, D), desmin (red; A, B), and laminin (red; C, D). Pictures were acquired by confocal laser scanning microscopy. Pericytes can be clearly identified by desmin staining and are present as expected at the periphery of the blood vessels (A, B; asterisks). Note that TNW staining is adjacent to the pericytes but does not encircle them (A). In contrast, TNC staining clearly encloses all pericytes present around the blood vessel (B). Laminin staining localizes the basement membrane shared by endothelial and pericytes cell layers (C, D). TNW is present only within the area delimited by the laminin staining (C), whereas TNC is not restricted to this basement membrane and clearly extends beyond the laminin staining (D). Scale bars = 10 μm .

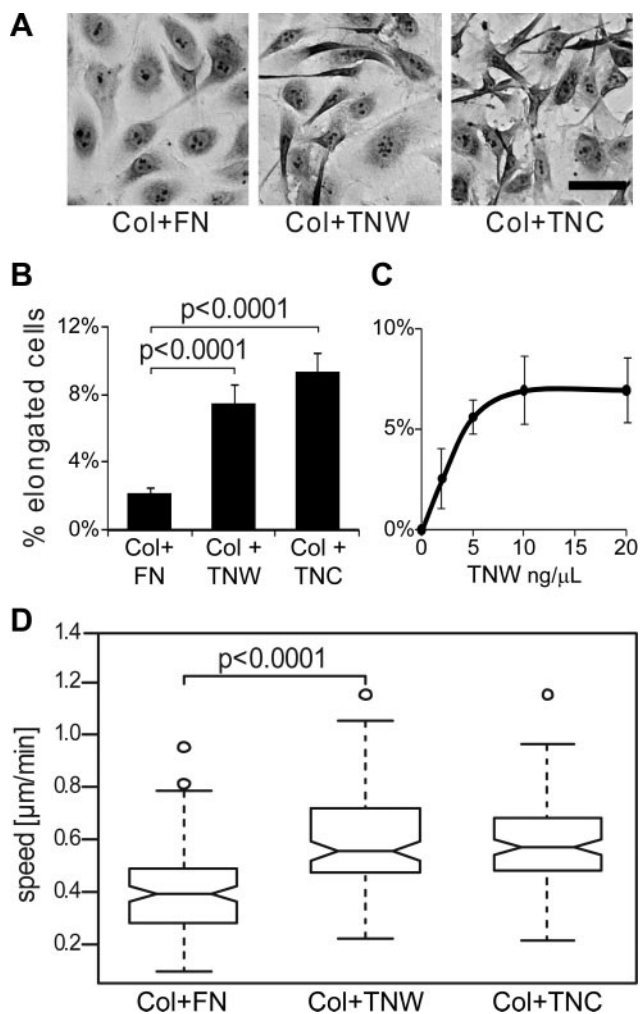


Figure 5. Morphology and motility of HUVECs seeded on fibronectin, tenascin-W, or tenascin-C in combination with type I collagen. **A)** Culture plates were coated with type I collagen, followed by fibronectin (FN), tenascin-W (TNW) or tenascin-C (TNC). HUVECs were seeded on these mixed substrata and incubated for 3 h at 37°C. Cells were then fixed and stained with crystal violet, and morphology of the cells was observed. Morphology of HUVEC populations observed on the different substrata is shown. Note the emergence of elongated cells in the presence of TNW and TNC. Scale bar = 50 μ m. **B)** Percentage of elongated cells on total number of adherent cells in each condition described in **A**. Statistical analyses were performed with ANOVA. **C)** Culture plates were coated with type I collagen. HUVECs were then seeded in serum-free medium containing increasing concentrations of soluble TNW or BSA as a control. After 3 h incubation at 37°C, cells were fixed, stained with crystal violet and analyzed. For each concentration of TNW, the number of HUVEC elongated cells was assessed, and the percentage of the total number of cells was calculated. Background, evaluated as percentage of HUVEC elongated cells observed in control conditions (*i.e.*, BSA at the same concentration), was then deduced. **D)** Culture plates were coated with type I collagen, followed by FN, TNW, or TNC. After 2 h of incubation at 37°C, the movement of HUVECs was recorded by time-lapse microscopy. Cell motility was quantified, tracking ≥ 35 cells/condition throughout the time stack. Results are represented with a box plot; thicker line represents median value. Ten percent of the values are composed within the notch surrounding the median line. Bottom and top extensions of the

ing tenascin-W strongly increased the sprouting capacity of HUVEC spheroids (Fig. 7B), thus confirming a proangiogenic role for tenascin-W.

DISCUSSION

In the present study, we found overexpression of tenascin-W in 80% of the glioma samples tested. In contrast, we could not detect tenascin-W in healthy human brain tissue, confirming previous studies in mice (21). This differential expression of tenascin-W in healthy brain *vs.* tumor tissues reveals a high potential for tenascin-W as a brain tumor biomarker. Our protein data paralleled an independent study on the transcript level performed by Bredel *et al.* (31). As yet we have no evidence that tenascin-W expression could be used as a predictor of the severity and the aggressiveness of gliomas, since oligodendrogliomas express tenascin-W to a similar extent as glioblastomas. Also, we were unable to find any correlation between patient survival data and the level of expression of tenascin-W, but extending the number of samples would be necessary to establish firmly whether a correlation exists.

Previous studies performed in our laboratory reported overexpression of tenascin-W, as well as tenascin-C in breast (22) and colon (23) tumors, two organs characterized by an absence of tenascin-W in normal, nonpathological conditions. In these carcinomas, the source of tenascin-C is the stromal or cancer-associated fibroblasts, shown to play an active role in the progression of the tumor (for review, see ref. 2). Like tenascin-C, tenascin-W is also present in the stroma of these carcinomas. The situation is different in glioblastomas and melanomas, in which the tumor cells themselves express tenascin-C. In contrast to tenascin-C, we could neither observe tenascin-W in brain cancer cells themselves after immunostaining glioma sections, nor detect expression of tenascin-W in the culture medium of glioma cell lines (data not shown). The present study shows that tenascin-W expression in gliomas is confined to blood vessels. Together with the induction of endothelial cell sprouting in *in vitro* functional angiogenesis assays, these observations point to a proangiogenic function of tenascin-W. This result is in agreement with a transcriptome study analyzing microvascular endothelial cells from patients suffering from impaired angiogenesis due to systemic sclerosis (39). *Tenascin-W* was among the genes down-regulated in these samples. Since proangiogenic features have also been described for tenascin-C in several studies (14, 16–18), our results reveal a common role between tenascin-C and tenascin-W. However, the blood vessel-associated expres-

box identify the first and the fourth quartile, respectively. Extreme lines represent the minimal and the maximal values of each dataset. Outliers are individually plotted as small circles. Note the significant increase ($P < 0.0001$, ANOVA test) of cell motility in the presence of TNW and TNC.

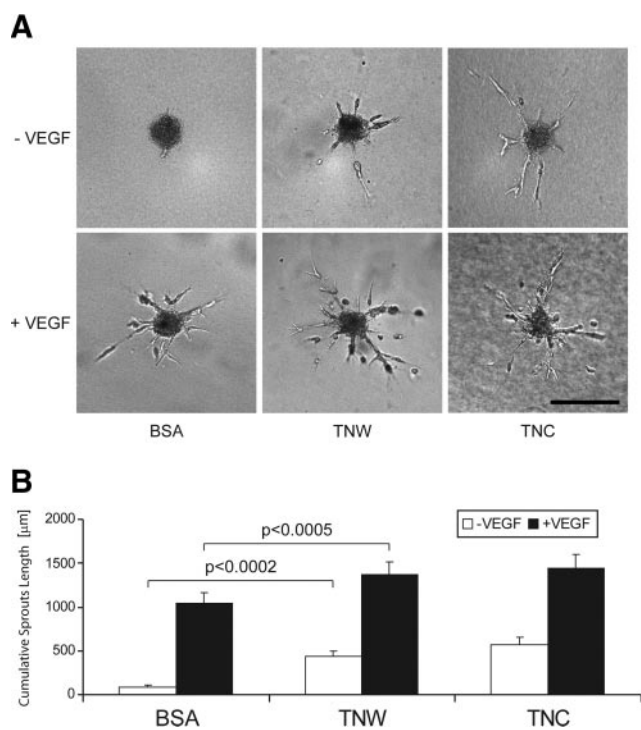


Figure 6. Sprouting capacity of HUVEC spheroids in a type I collagen gel containing purified tenascin-W and tenascin-C. HUVEC spheroids were added in a type I collagen gel containing BSA, tenascin-W (TNW), or tenascin-C (TNC) at a concentration of 20 µg/ml. Cultures were fed with endothelial growth medium in the presence or absence of VEGF at a concentration of 10 ng/ml (+VEGF or -VEGF, respectively). After 48 h, pictures of 10 randomly chosen spheroids/condition were acquired. A) Representative pictures of each condition. Scale bar = 200 µm. B) CSLs were quantified, measuring the total length of all sprouting processes originating from a single spheroid. Note the significant increase of HUVEC sprouting capacity in the presence of both TNW and TNC. This holds true in the absence of VEGF (open bars), as well as in the presence of VEGF (solid bars).

sion pattern of tenascin-W and tenascin-C differs slightly. Tenascin-C and tenascin-W are not solely restricted to the blood vessels themselves but are also visible in the perivascular space. Tenascin-C can be detected in association with desmin-positive pericytes, while tenascin-W was interior of the desmin-stained cells and seemed to be associated with endothelial cells. This suggests different cellular sources of the two proteins, such as pericytes for the production of tenascin-C and endothelial cells as the source of tenascin-W. This is supported by the observation that pericytes can secrete tenascin-C *in vitro* (data not shown), and *tenascin-W* transcripts have been observed in endothelial cells (39). The distinct expression patterns of tenascin-C and tenascin-W may, in addition, reveal specificities in the regulation of each tenascin. Some glioblastomas express both tenascins, some express either tenascin-C or tenascin-W, and some of them express neither. Unfortunately, analysis of clinical data did not enable us to link any of these combinations with a given patient outcome. Considering that tenascin-C and tenascin-W may be regulated differently, that bone morphogenic proteins (BMPs) mainly induce tenascin-W (21, 40), and

that several BMP members promote angiogenesis in tumors (41–43), we postulate that tenascin-W could be a mediator of BMP activity in tumors.

Our results uncover a potential target for anticancer therapy. There are two ways ECM cancer markers can be used to combat cancer. First, they can be targeted directly. For example, decreasing the expression of tenascin-C by RNA interference was shown to inhibit metastasis of breast cancer cells in a xenograft model (19). Second, the

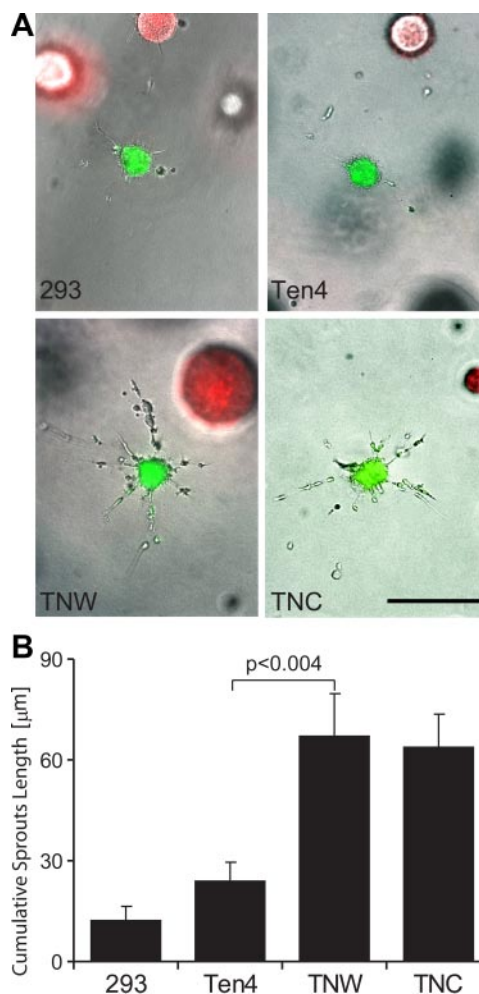


Figure 7. Sprouting capacity of HUVEC spheroids cocultured with HEK-293 cells secreting tenascin-W or tenascin-C in a type I collagen gel. A) HUVEC spheroids were combined in a type I collagen gel with HEK-293 spheroids in the presence of 10 ng/ml VEGF. HUVEC and HEK-293 spheroids were prepared with cells beforehand marked with DiO (green) and DiI (red) dyes, respectively. HEK-293 cells used in these experiments were stably transfected to express an empty plasmid (293), a teneurin-4 construct (Ten4), tenascin-W (TNW), or tenascin-C (TNC). Note that the sprouting capacity of HUVEC spheroids is increased only in the vicinity of 293 cells secreting TNW or TNC. Scale bar = 200 µm. B) HUVEC spheroids were added to type I collagen gels populated with dissociated HEK-293. After 48 h, pictures of 10 randomly chosen spheroids/condition were acquired. CSLs were quantified, measuring the total length of all sprouting processes originating from a single spheroid. Note that inclusion of HEK-293 cells secreting TNW and TNC significantly increased the sprouting capacity of HUVEC spheroids.

more extensively used approach is to use cancer-specific ECM proteins as “tumor flags” for the selective delivery of anticancer drugs at the site of the tumor (for review, see ref. 44). In the case of tenascin-C, such an approach has been successfully applied to brain cancer patients for many years (45, 46). The use of antibodies against the spliced isoform of tenascin-C containing extradomain C (47, 48) has led to enhanced tumor imaging and to a significant accumulation of therapeutic compounds in tumors in xenograft models. Furthermore, coupling of antibodies recognizing tenascin-C to interleukin-2 was reported to enhance the potency of chemotherapy in xenograft models of human breast cancer (49). Most important, the *in vivo* accessibility of fibronectin with extra domain B was confirmed in three lymphoma patients, in which radioimmunotherapy induced a sustained partial remission in relapsed lymphoma patients, proving the efficacy of this method (50).

On the basis of the results presented in this study, tenascin-W should be considered as a novel molecule with potential for diagnostic (imaging) or therapeutic applications since it is overexpressed in most of the gliomas, but not in healthy tissues; it is localized immediately surrounding endothelial cells and thus readily reached by the circulation; and its positive effect on angiogenesis might be neutralized by such treatments. **[F]**

Grant support is provided by the Schweizerische Nationalfonds (SNF), National Center for Competence in Research (C.R.), Oncosuisse OCS-01613-12-2004 (A.M.), SNF 3100A0-120235 (R.C.-E.), and Krebsliga beider Basel 20-2008 (F.B.). We thank Gregory Bieler (Division of Experimental Oncology, University of Lausanne, Lausanne, Switzerland) for kindly providing us early passages of HUVECs, Natsuko Imaizumi and Eveline Faes for their technical expertise with angiogenesis assays, Catherine Schiltz and Sandrine Bichet for their help with immunohistochemistry, Daniela Kenzelmann (FMI, Basel, Switzerland) for the teneurin-4 constructs, Laurent Gelman for his help with microscopy, and Clare Isacke (Institute of Cancer Research, London, UK) for the culture medium of pericytes. We also thank Rémi Terranova and Richard P. Tucker for critical reading of the manuscript.

REFERENCES

- Bhowmick, N. A., Neilson, E. G., and Moses, H. L. (2004) Stromal fibroblasts in cancer initiation and progression. *Nature* **432**, 332–337
- Kalluri, R., and Zeisberg, M. (2006) Fibroblasts in cancer. *Nat. Rev. Cancer* **6**, 392–401
- Lorusso, G., and Rugg, C. (2008) The tumor microenvironment and its contribution to tumor evolution toward metastasis. *Histochem. Cell Biol.* **130**, 1091–1103
- Kass, L., Erler, J. T., Dembo, M., and Weaver, V. M. (2007) Mammary epithelial cell: influence of extracellular matrix composition and organization during development and tumorigenesis. *Int. J. Biochem. Cell Biol.* **39**, 1987–1994
- Plate, K. H., Breier, G., Weich, H. A., and Risau, W. (1992) Vascular endothelial growth factor is a potential tumour angiogenesis factor in human gliomas *in vivo*. *Nature* **359**, 845–848
- Tuxhorn, J. A., McAlhany, S. J., Yang, F., Dang, T. D., and Rowley, D. R. (2002) Inhibition of transforming growth factor-beta activity decreases angiogenesis in a human prostate cancer-reactive stroma xenograft model. *Cancer Res.* **62**, 6021–6025
- Kalas, W., Yu, J. L., Milsom, C., Rosenfeld, J., Benezra, R., Bornstein, P., and Rak, J. (2005) Oncogenes and Angiogenesis: down-regulation of thrombospondin-1 in normal fibroblasts exposed to factors from cancer cells harboring mutant ras. *Cancer Res.* **65**, 8878–8886
- Brellier, F., Tucker, R. P., and Chiquet-Ehrismann, R. (2009) Tenascins and their implications in diseases and tissue mechanics. *Scand. J. Med. Sci. Sports* **19**, 511–519
- Chiquet-Ehrismann, R., Mackie, E. J., Pearson, C. A., and Sakakura, T. (1986) Tenascin: an extracellular matrix protein involved in tissue interactions during fetal development and oncogenesis. *Cell* **47**, 131–139
- Orend, G., and Chiquet-Ehrismann, R. (2006) Tenascin-C induced signaling in cancer. *Cancer Lett.* **244**, 143–163
- Huang, W., Chiquet-Ehrismann, R., Moyano, J. V., Garcia-Pardo, A., and Orend, G. (2001) Interference of tenascin-C with syndecan-4 binding to fibronectin blocks cell adhesion and stimulates tumor cell proliferation. *Cancer Res.* **61**, 8586–8594
- Herold-Mende, C., Mueller, M. M., Bonsanto, M. M., Schmitt, H. P., Kunze, S., and Steiner, H. H. (2002) Clinical impact and functional aspects of tenascin-C expression during glioma progression. *Int. J. Cancer* **98**, 362–369
- De Wever, O., Nguyen, Q. D., Van Hoorde, L., Bracke, M., Bruyneel, E., Gelpi, C., and Mareel, M. (2004) Tenascin-C and SF/HGF produced by myofibroblasts *in vitro* provide convergent pro-invasive signals to human colon cancer cells through RhoA and Rac. *FASEB J.* **18**, 1016–1018
- Ishiwata, T., Takahashi, K., Shimizu, Y., Ohashi, R., Cui, R., Takahashi, F., Shimizu, K., Miura, K., and Fukuchi, Y. (2005) Serum tenascin-C as a potential predictive marker of angiogenesis in non-small cell lung cancer. *Anticancer Res.* **25**, 489–495
- Saito, Y., Shiota, Y., Nishisaka, M., Owaki, T., Shimamura, M., and Fukai, F. (2008) Inhibition of angiogenesis by a tenascin-c peptide which is capable of activating beta1-integrins. *Biol. Pharm. Bull.* **31**, 1003–1007
- Tanaka, K., Hiraawa, N., Hashimoto, H., Yamazaki, Y., and Kusakabe, M. (2004) Tenascin-C regulates angiogenesis in tumor through the regulation of vascular endothelial growth factor expression. *Int. J. Cancer.* **108**, 31–40
- Schenk, S., Chiquet-Ehrismann, R., and Battagay, E. J. (1999) The fibrinogen globe of tenascin-C promotes basic fibroblast growth factor-induced endothelial cell elongation. *Mol. Biol. Cell* **10**, 2933–2943
- Zagzag, D., Shiff, B., Jallo, G. I., Greco, M. A., Blanco, C., Cohen, H., Hukin, J., Allen, J. C., and Friedlander, D. R. (2002) Tenascin-C promotes microvascular cell migration and phosphorylation of focal adhesion kinase. *Cancer Res.* **62**, 2660–2668
- Tavazoie, S. F., Alarcon, C., Oskarsson, T., Padua, D., Wang, Q., Bos, P. D., Gerald, W. L., and Massague, J. (2008) Endogenous human microRNAs that suppress breast cancer metastasis. *Nature* **451**, 147–152
- Calvo, A., Catena, R., Noble, M. S., Carbott, D., Gil-Bazo, I., Gonzalez-Moreno, O., Huh, J. I., Sharp, R., Qiu, T. H., Anver, M. R., Merlino, G., Dickson, R. B., Johnson, M. D., and Green, J. E. (2008) Identification of VEGF-regulated genes associated with increased lung metastatic potential: functional involvement of tenascin-C in tumor growth and lung metastasis. *Oncogene* **27**, 5373–5384
- Scherberich, A., Tucker, R. P., Samandari, E., Brown-Luedi, M., Martin, D., and Chiquet-Ehrismann, R. (2004) Murine tenascin-W: a novel mammalian tenascin expressed in kidney and at sites of bone and smooth muscle development. *J. Cell Sci.* **117**, 571–581
- Degen, M., Brellier, F., Kain, R., Ruiz, C., Terracciano, L., Orend, G., and Chiquet-Ehrismann, R. (2007) Tenascin-W is a novel marker for activated tumor stroma in low-grade human breast cancer and influences cell behavior. *Cancer Res.* **67**, 9169–9179
- Degen, M., Brellier, F., Schenk, S., Driscoll, R., Zaman, K., Stupp, R., Tornillo, L., Terracciano, L., Chiquet-Ehrismann, R., Rugg, C., and Seelentag, W. (2008) Tenascin-W, a new marker of cancer stroma, is elevated in sera of colon and breast cancer patients. *Int. J. Cancer* **122**, 2454–2461
- Lino, M., and Merlo, A. (2009) Translating biology into clinic: the case of glioblastoma. *Curr. Opin. Cell Biol.* **21**, 311–316
- Cairncross, J. G. (1998) Cognition in survivors of high-grade glioma. *J. Clin. Oncol.* **16**, 3210–3211

26. Orend, G. (2005) Potential oncogenic action of tenascin-C in tumorigenesis. *Int. J. Biochem. Cell. Biol.* **37**, 1066–1083
27. Zamecnik, J. (2005) The extracellular space and matrix of gliomas. *Acta Neuropathol.* **110**, 435–442
28. Sivasankaran, B., Degen, M., Ghaffari, A., Hegi, M. E., Hamou, M. F., Ionescu, M. C., Zweifel, C., Tolnay, M., Wasner, M., Mergenthaler, S., Miserez, A. R., Kiss, R., Lino, M. M., Merlo, A., Chiquet-Ehrismann, R., and Boulay, J. L. (2009) Tenascin-C is a novel RBPJ κ -induced target gene for Notch signaling in gliomas. *Cancer Res.* **69**, 458–465
29. Leins, A., Riva, P., Lindstedt, R., Davidoff, M. S., Mehraein, P., and Weis, S. (2003) Expression of tenascin-C in various human brain tumors and its relevance for survival in patients with astrocytoma. *Cancer* **98**, 2430–2439
30. Reardon, D. A., Zalutsky, M. R., and Bigner, D. D. (2007) Antitenascin-C monoclonal antibody radioimmunotherapy for malignant glioma patients. *Expert Rev. Anticancer Ther.* **7**, 675–687
31. Bredel, M., Bredel, C., Juric, D., Harsh, G. R., Vogel, H., Recht, L. D., and Sikić, B. I. (2005) Functional network analysis reveals extended gliomagenesis pathway maps and three novel MYC-interacting genes in human gliomas. *Cancer Res.* **65**, 8679–8689
32. Orend, G., Huang, W., Olayioye, M. A., Hynes, N. E., and Chiquet-Ehrismann, R. (2003) Tenascin-C blocks cell-cycle progression of anchorage-dependent fibroblasts on fibronectin through inhibition of syndecan-4. *Oncogene* **22**, 3917–3926
33. Fischer, D., Tucker, R. P., Chiquet-Ehrismann, R., and Adams, J. C. (1997) Cell-adhesive responses to tenascin-C splice variants involve formation of fascin microspikes. *Mol. Biol. Cell* **8**, 2055–2075
34. Korff, T., and Augustin, H. G. (1998) Integration of endothelial cells in multicellular spheroids prevents apoptosis and induces differentiation. *J. Cell Biol.* **143**, 1341–1352
35. Korff, T., and Augustin, H. G. (1999) Tensional forces in fibrillar extracellular matrices control directional capillary sprouting. *J. Cell Sci.* **112**, 3249–3258
36. Ivanov, D., Philippova, M., Tkachuk, V., Erme, P., and Resink, T. (2004) Cell adhesion molecule T-cadherin regulates vascular cell adhesion, phenotype and motility. *Exp. Cell Res.* **293**, 207–218
37. Romer, L. H., McLean, N., Turner, C. E., and Burridge, K. (1994) Tyrosine kinase activity, cytoskeletal organization, and motility in human vascular endothelial cells. *Mol. Biol. Cell* **5**, 349–361
38. Canfield, A. E., and Schor, A. M. (1995) Evidence that tenascin and thrombospondin-1 modulate sprouting of endothelial cells. *J. Cell Sci.* **108**, 797–809
39. Giusti, B., Fibbi, G., Margheri, F., Serrati, S., Rossi, L., Poggi, F., Lapini, I., Magi, A., Del Rosso, A., Cinelli, M., Guiducci, S., Kahaleh, B., Bazzichi, L., Bombardieri, S., Matucci-Cerinic, M., Gensini, G. F., Del Rosso, M., and Abbate, R. (2006) A model of anti-angiogenesis: differential transcriptome profiling of microvascular endothelial cells from diffuse systemic sclerosis patients. *Arthritis Res. Ther.* **8**, R115
40. Kimura, H., Akiyama, H., Nakamura, T., and de Crombrughe, B. (2007) Tenascin-W inhibits proliferation and differentiation of preosteoblasts during endochondral bone formation. *Biochem. Biophys. Res. Commun.* **356**, 935–941
41. Langenfeld, E. M., and Langenfeld, J. (2004) Bone morphogenetic protein-2 stimulates angiogenesis in developing tumors. *Mol. Cancer Res.* **2**, 141–149
42. Ren, R., Charles, P. C., Zhang, C., Wu, Y., Wang, H., and Patterson, C. (2007) Gene expression profiles identify a role for cyclooxygenase 2-dependent prostanoid generation in BMP6-induced angiogenic responses. *Blood* **109**, 2847–2853
43. Rothhammer, T., Bataille, F., Spruss, T., Eissner, G., and Bosserhoff, A. K. (2007) Functional implication of BMP4 expression on angiogenesis in malignant melanoma. *Oncogene* **26**, 4158–4170
44. Kaspar, M., Zardi, L., and Neri, D. (2006) Fibronectin as target for tumor therapy. *Int. J. Cancer.* **118**, 1331–1339
45. Bigner, D. D., Brown, M. T., Friedman, A. H., Coleman, R. E., Akabani, G., Friedman, H. S., Thorstad, W. L., McLendon, R. E., Bigner, S. H., Zhao, X. G., Pegram, C. N., Wikstrand, C. J., Herndon, J. E., 2nd, Vick, N. A., Paleologos, N., Cokgor, I., Provenzale, J. M., and Zalutsky, M. R. (1998) Iodine-131-labeled antitenascin monoclonal antibody 81C6 treatment of patients with recurrent malignant gliomas: phase I trial results. *J. Clin. Oncol.* **16**, 2202–2212
46. De Santis, R., Anastasi, A. M., D'Alessio, V., Pelliccia, A., Albertoni, C., Rosi, A., Leoni, B., Lindstedt, R., Petronzelli, F., Dani, M., Verdoliva, A., Ippolito, A., Campanile, N., Manfredi, V., Esposito, A., Cassani, G., Chinol, M., Paganelli, G., and Carminati, P. (2003) Novel antitenascin antibody with increased tumour localisation for pretargeted antibody-guided radioimmunotherapy (PAGRIT). *Br. J. Cancer.* **88**, 996–1003
47. Silacci, M., Brack, S. S., Spath, N., Buck, A., Hillinger, S., Arni, S., Weder, W., Zardi, L., and Neri, D. (2006) Human monoclonal antibodies to domain C of tenascin-C selectively target solid tumors in vivo. *Protein Eng. Des. Sel.* **19**, 471–478
48. Brack, S. S., Silacci, M., Birchler, M., and Neri, D. (2006) Tumor-targeting properties of novel antibodies specific to the large isoform of tenascin-C. *Clin. Cancer Res.* **12**, 3200–3208
49. Marlind, J., Kaspar, M., Trachsel, E., Somavilla, R., Hindle, S., Bacci, C., Giovannoni, L., and Neri, D. (2008) Antibody-mediated delivery of interleukin-2 to the stroma of breast cancer strongly enhances the potency of chemotherapy. *Clin. Cancer Res.* **14**, 6515–6524
50. Sauer, S., Erba, P. A., Petrini, M., Menrad, A., Giovannoni, L., Grana, C., Hirsch, B., Zardi, L., Paganelli, G., Mariani, G., Neri, D., Durkop, H., and Menssen, H. D. (2009) Expression of the oncofetal ED-B-containing fibronectin isoform in hematologic tumors enables ED-B-targeted 131I-L19SIP radioimmunotherapy in Hodgkin lymphoma patients. *Blood* **113**, 2265–2274

Received for publication June 26, 2009.
Accepted for publication October 8, 2009.